The Framework for a Neutral Hydrogen Map of the Outer Galaxy Using Asteroseismic Distances

Luke Benavitz[a], Sukanya Chakrabarti[b], Daniel Hey[a], Daniel Huber[a]

[a]*Institute for Astronomy, University of Hawai'i, 2680 Woodlawn Drive, Honolulu, HI 96822, USA*
[b]*School of Physics and Astronomy, Rochester Institute of Technology, 84 Lomb Memorial Drive, Rochester, NY*

Abstract

We present a framework to derive the dense neutral atomic hydrogen (HI) map of the Galaxy using asteroseismic distances, which are more precise than kinematic distances. By matching patterns in the line-of-sight velocity as a function of galactic longitude, $v_{LSR}(l)$, for stars with asteroseismic distances and the HI LAB data, we determine where the HI gas is along a particular line of sight. By comparing and matching features in this domain, we can make use of asteroseismic distances without any intermediate use of kinematic distances. Using data from *Gaia*, we find there is a pattern in the $v_{LSR}(l)$ data of young Cepheid variables that is similar to that seen in the HI LAB data. We show also that the pattern becomes more diffuse and less recognizable for older stars. We superimpose the distances of Cepheid variables onto the previously derived HI surface density map to analyze the structure and tidal disturbances in the HI disk. We also analyzed a Smoothed Particle Hydrodynamics simulation of the Milky Way and find that the patterns in the gas and young stars are correlated in $v_{LSR}(l)$. Future work will include overlaying distances of spiral arms in the simulated galaxy on the $v_{LSR}(l)$ plot to provide a proof of principle of the method.

Keywords: Galaxy: disk — Galaxy: kinematics and dynamics — Galaxy: structure — ISM: structure — radio lines: general

1. Introduction

The topography of the gas disk of the Milky Way (MW) has been extensively mapped using kinematic distances (Bon-Chul Koo et al., 2017). The kinematic method is commonly used to determine the distances to gas clouds, like high-mass star-forming regions, in the study of Galactic structure (Wenger et al., 2018). Kinematic distances are derived by measuring the local standard of rest (LSR) velocity, v_{LSR}, of an object while assuming a model of Galactic rotation (Bon-Chul Koo et al., 2017). If the object is on a circular orbit following this Galactic rotation model, then the LSR velocity of the object uniquely identifies the object's

Email address: lukefb@hawaii.edu (Luke Benavitz)

Galactocentric radius, R. Beyond the solar orbit around the galactic center, this technique also uniquely determines the object's Galacto- centric azimuth, θ. Within the solar orbit around the galactic center, a single LSR velocity may correspond to two distances, leading to a kinematic ambiguity: a "near" and "far" kinematic distance. We must use additional information to identify the kinematic distance ambiguity resolution.

HI maps are maps of the MW made with 21cm HI surveys, and they can be analyzed to characterize the tidal disturbances of the gas disk of the MW and help us understand the MW's merger history and possible past merger candidates (Weinberg and Blitz, 2006; Chakrabarti and Blitz, 2009, 2011; Chakrabarti, 2013). An example of a dominant tidal disturbance is warping. Warping occurs when there is vertical displacement in or out of the plane of the galaxy and when there is planar disturbances in the HI. These disturbances can be analyzed to make predictions about how the MW behaves, and what could be affecting it (Weinberg and Blitz, 2006). The HI disk of the Galaxy also manifests large planar disturbances. By analyzing the planar HI disturbances Sukanya Chakrabarti and Leo Blitz (2009) predicted the existence and location of a new dwarf galaxy. Later analysis by Chakrabarti et al. (2019) indicates that the recently discovered Antlia 2 dwarf galaxy, which has similar properties to the earlier predicted dwarf galaxy, may be the culprit that produced the large pertubations in the HI disk. The warps in the gas disk of the MW have been known since 1957 (KERR, F. et al., 1957). This warp is asymmetric in galactocentric coordinates: in the northern data, the warp has an amplitude that rises higher than 4kpc above the galactic plane at the galactocentric radius of 25kpc, while the southern data indicates that the warp falls to an amplitude of around 1kpc below the galactic plane.

Studying other galaxies can also help us understand how the MW behaves. At least half of all galaxies are warped, and galaxies with smaller dark matter halo core radii are less likely to be warped (Levine et al., 2006). We also see that a warp's line of nodes starts out straight and at a transition begins to advance in the direction of rotation, with some exceptions. It is also shown that in galaxies where the HI gas extends past the optical components are more commonly warped, and on top of that, are more commonly warped asymmetrically. In the MW, there are many other influences that encourage warping, some of which include: dust, carbon monoxide (CO), solar neighborhood stars, and Infrared Astronomical Satellite (IRAS) point sources.

A challenge with kinematic distances is that they are very uncertain. An alternative is asteroseismology. Asteroseismic distances involve utilizing stellar oscillations (Auge et al., 2020). In a broad sense, larger and more luminous stars oscillate at lower frequencies, and by finding these lower frequencies, we can determine the luminosity of the star. We can use light curves to show the relative brightness of stars with respect to time, and these variation can arise from stellar oscillations. Given the intrinsic luminosity, we can determine the distance (Auge et al., 2020). An example of asteroseismic distanced stars are Cepheid variable stars. Asteroseismic distance measurements are better than kinematic distances because asteroseismic distances have distance errors of 15%, as shown by

Auge et al. (2020), while kinematic distanes have errors of 30% as shown by Ralph Schonrich et al. (2012). Asteroseismic distances has half the error that kinematic distancing produces, so using asteroseismic distances to map the MW will be far superior to kinematic distances citepConnorAuge2020,RalphSchonrich2012. In this paper we have produced a framework to rederive the HI map of the Milky Way using asteroseismic distances, which would produce a much more accurate map than ever before. This more accurate map will help us to better characterize the tidal disturbances of the gas disk of the MW and help us understand the MW's merger history and possible past merger candidates. It will also help to better constrain the structure of the MW.

2. Method

2.1. Data Processing

The most widely used HI survey data sets are the 21cm Effelsberg-Bonn HI survey (EBHIS), Galactic All Sky Survey (GASS), and Leiden/Argentine/Bonn (LAB) survey (Levine et al., 2006). Of these, the LAB survey is the most commonly used. We describe the 21 cm LAB data here briefly. LAB data can be used to conduct a quantitative study of the disturbances in HI, like warping and the ripples in the plane of the disk. The LAB survey is a combination of the Leiden-Dwingeloo Survey (LDS) data set with Southern sky observations from the Instituto Argentino de Radioastronomia; however, much attention has been paid toward ensuring a uniform data set. The combined survey maps the entire sky within -450 kms^{-1} v_r 400 kms^{-1}, with a resolution of 1.3 kms^{-1}; this velocity range includes all of the gas in the MW in circular rotation. The data is also Hanning smoothed which has a velocity resolution of 1.9 kms^{-1}, and it only looks at the data where a vast majority of the HI gas is: *jbj* 30^0. Roughly the entirety of the warps in the MW's disk lies within this range.

The LAB data is given in celestial galactic coordinates: longitude, latitude, and radial velocity (l, b, v_r). To convert to galactocentric cylindrical coordinates we make use of standard coordinate transformation equations which gets our data from (l, b, v_r) to galactocentric cylindrical coordinates (R, ϕ, z) where R is the radius away from the center of mass of the galaxy, ϕ is the galactic rotation curve, and z is the the distance in and out of the plane of the MW. R_0 is 8.5kpc which is the distance from the Sun to the galactic center, r' is the projection onto the plane of the disk of the vector connecting the Sun's location to the point under investigation, Φ_0 is $220kms^{-1}$ which is the speed the Sun orbits around the galactic center, and v_{II} is a parameterization of the ellipticity of the galactocentric orbit, which is free to vary with galactocentric radius. We will focus on the topography of the HI map of the MW, so we only work with r and ϕ.

2.2. Spiral structure in the young stars and the gas

We can expect that the MW's HI gas will have a similar spiral pattern as the young stars because the spiral structure in the young stars as seen in blue light is similar to that of the gas in external galaxies (Sukanya Chakrabarti et al., 2003). Stars that are younger have sharp, distinct spiral arms in blue light while older stars have more diffuse spiral arms as seen in red light

(Sukanya Chakrabarti et al., 2003). We first use the LAB data to make a top down contour plot of the surface density as a function of Galactocentric radius R and ϕ [fig 2]. We then superimpose the locations of Cepheid variable stars for 2431 Galactic Cepheids, most of which were discovered by the fourth phase of the Optical Gravitational Lensing Experiment (OGLE-IV) project (A. Udalski1 et al., 2015), onto the contour map in order to get more accurate distances in the map. We choose Cepheids because they are young stars that formed in the spiral arms of the MW where the majority of the HI gas also resides (Sukanya Chakrabarti et al., 2003). We plot Cepheids of ages between 29Myr to 209Myr, as explained the the description of figure 1. We then overplot a logarithmic spiral onto the map, and this spiral should follow the shape of the spiral that the Cepheids make because they formed once the MW's arms were already formed. The resulting plot is shown in Figure 2.

We exclude all points that lie within 345^0 l 15^0 or 165^0 l 195^0. Points in these two wedges have velocities along the line of sight that are too small with respect to their random velocities to establish reliable kinematic distances. All points in this region are set to $T_b = 0$ where T_b is the brightness temperature of the HI gas.

2.3. The natural space for HI: (l, v) diagrams

Traditionally, HI gas in the Milky Way is displayed with (l, v_{LSR}) diagrams. No distance information is present in the LAB map, so kinematic distances are assumed to produce projected surface density maps in which there are inherent distance uncertainties (Kalberla et al., 2005). These uncertainties arise from the adopted Galactic rotation curve, the non-circular motions due to streaming along the spiral arms, and velocity crowding (Burton W. B., 1971). These problems are most severe for the inner Galaxy where the line of sight crosses tangential points, leading to an ambiguity in distance occurs for a given LSR velocity. As previously stated, this is why making a (l, v_{LSR}) diagram is so important: to bypass these uncertainties (Burton W. B., 1971). Stars on the other hand do have distances (of one kind or another), so it is more uncommon to see stellar (l, v_{LSR}) diagrams.

We produce (l, v_{LSR}) diagrams for young stars so that we may pattern match the features in the natural space for HI gas. Pattern matching is taking specific (l, v_{LSR}) values that correspond to a star with a distance while also looking at the corresponding region of gas with the same (l, v_{LSR}) values. The distance to the star at (l, v_{LSR}) can be given to the region of gas at (l, v_{LSR}), thus dynamically coupling the young stars and HI through (l, v_{LSR}) diagrams. It is more useful to use younger stars, like Cepheids, in these diagrams because these stars will have formed in the spirals of the MW. The gas in the MW is condensed in the spiral arms as well, so younger stars and HI in the LAB data will be in the same region of space which should cause the (l, v_{LSR}) plots of these two respectively to have the same shape and patterns.

2.4. Simulated Data

We next analyzed a Smoothed Particle Hydrodynamics simulation of the Milky Way, and we make our (l, v) diagrams using the GASOLINE code that produces simulated MW data (Wadsley et al., 2004). The simulation data contains information about stars

of various ages which we categorize as old, young, and fresh stars. The timescale is adjusted so that present day is 0Myr, and negative years are stars that have formed in the past. We define old stars as stars with ages from -100Myr to 0MYr, young stars range between 0Myr to 13Myr of age, fresh stars range from 0 to 50 Myr of age. We limit the simulation data so that all stars should range between -100Myr to 100Myr of age. We also use data from the same simulation for CO, and we can see the (l, v) diagram for CO in figure **??**.

3. Results and Discussion

3.1. HI and Stellar Dynamic Coupling

In figure 2, we find that the overlaid logarithmic spiral arm on top of the HI surface density map aligns with the spiral arm structure that both the Cepheid variable stars and HI reside in. This reinforces the idea that young stars, like young Cepheid variables in out age cut, and HI gas should reside in the spiral structures of the MW. It reconfirms that young stars and HI are easily detected to be in the same region of space.

3.2. (l, v) diagram

In figure 3, the bottom plot is the (l, v_{LSR}) plot for young stars from Gaia Data Release 3. They have an upper limit on ages of 400Myr, and this upper limit was used by using a comprable upper limit similar to that of the Cepheid variable stars. It is easy to see the motivation behind this age by looking at figure 1. We can also see what happens if we use stars of any ages by looking at figure 4, and it is easy to be seen that the pattern becomes more diffuse and less recognizable for older stars when trying to pattern match for HI. We see that the (l, v) diagram for both the simulated CO in figure **??** and for the HI in the top of figure 3 can undergo pattern matching with figure 5b. We can then take a point in that pattern, in other words a star, and get this stars l and v data. We then see that we are able to extract put the star's distance on that specific point in the HI and CO gas.

We find that the HI and young star's (l, v_{LSR}) plots can be pattern matched. The HI gas possess (l, v_{LSR}) information, but no distance information. The young stars possess (l, v_{LSR}) information and distance information, whether it be from asteroseismic distancing or some other method. We can then take (l, v_{LSR}) information from a young star, take the exact same region of HI gas at that (l, v_{LSR}) and give that region of HI gas that star's distance. This shows that HI and young stars are dynamically coupled, and young star's distances can be given to HI, thus giving a distance to that point of HI. This is pattern matching.

4. Conclusions

1. We find similar patterns in the face-on projected surface density map of the neutral hydrogen gas and in young Cepheid variables stars. By mining the Gaia DR3 dataset, we see also similar patterns in the gas and the young stars in $v_{LSR}(l)$, while there are no clear patterns in the old stars.
2. We have analyzed a Smoothed Particle Hydrodynamics simulation and here also we find that structures in the gas and young stars are correlated in

$v_{LSR}(l)$ space, while there are no recognizable structures in the old stars.

3. We can find distances to points in the HI by finding stars with longitude and radial velocity information, matching that information to a point in the HI and giving that point of HI the same distance as the matched star.
4. Pattern matching (l, v_{LSR}) diagrams is a viable method for using asteroseismic distances to re-derive the HI map of the MW. Here, we have demonstrated this concept using a SPH simulation, and will apply it in the future to stars with asteroseismic distances.

We can use asteroseismic distances, without any intermediate use of kinematic distances, to M giants and eclipsing binaries, when that data becomes available, and the 21cm LAB data to rederive a neutral hydrogen map of the MW and conduct a quantitative study of the disturbances in HI, like warping. We can use this more accurate HI map to see constrain interactions with dwarf galaxies and understand the formation of the warp and the large planar disturbances in the gas disk. We will also be able to better understand the characteristics other spiral galaxies like the MW. We will also be able to better constrain parameters like the the amount of dark matter in the MW.

Acknowledgements

Sukanya Charkrabarti, Daniel Hey, and Daniel Huber helped with the coding and conceptualization of this framework with the intentino of using asteroseismic distancing in the future.

For this Summer 2022 University of Hawaii at Manoa REU program:

1. LB acknowledges support from Research Experience for Undergraduate program at the Institute for Astronomy, University of Hawaii-Manoa funded through NSF grant #6109694.
2. LB would like to thank the Institute for Astronomy for their hospitality during the course of this project.

References

A. Udalski1, M.K. Szyman ski, and G. Szyman ski. OGLE-IV: Fourth Phase of the Optical Gravitational Lensing Experiment. *ACTA ASTRONOMICA*, page 38, Apr. 2015.

C. Auge, D. Huber, A. Heinze, B. J. Shappee, J. Tonry, S. Chakrabarti, R. E. Sanderson, L. Denneau, H. Flewelling, T. W. S. Holoien, C. S. Kochanek, G. Pignata, A. Sickafoose, B. Stalder, K. Z. Stanek, D. Stello, and T. A. Thompson. Beyond Gaia: Asteroseismic Distances of M Giants Using Ground-based Transient Surveys. AJ, 160(1):18, July 2020. doi: 10.3847/1538-3881/ab91bf.

Bon-Chul Koo, Geumsook Park1, Woong-Tae Kim, Myung Gyoon Lee, Dana S. Balser, and Trey V. Wenger. Tracing the Spiral Structure of the Outer Milky Way with Dense Atomic Hydrogen Gas. *The Astronomical Society of the Pacific*, page 19, June 2017.

Burton W. B. Galactic Structure Derived from Neutral Hydrogen Observations Using Kinematic Models Based on the Density-wave Theory. *Astronomy and Astrophysics*, page 21, Jan. 1971.

S. Chakrabarti. Deciphering the Dynamical Echoes of Dwarf Galaxies on the Milky Way Disk. In *American Astronomical Society Meeting Abstracts*, volume 222 of *American Astronomical Society Meeting Abstracts*, page 203.03, June 2013.

S. Chakrabarti and L. Blitz. Tidal imprints of a dark subhalo on the outskirts of the Milky Way. MNRAS, 399(1):L118–L122, Oct. 2009. doi: 10.1111/j.1745-3933.2009.00735.x.

S. Chakrabarti and L. Blitz. Tidal Imprints of a Dark Sub-halo on the Outskirts of the Milky Way. II. Perturber Azimuth. ApJ, 731(1):40, Apr. 2011. doi: 10.1088/0004-637X/731/1/40.

S. Chakrabarti, P. Chang, A. M. Price-Whelan, J. Read, L. Blitz, and L. Hernquist. Antlia 2's Role in Driving the Ripples in the Outer Gas Disk of the Galaxy. ApJ, 886(1):67, Nov. 2019. doi: 10.3847/1538-4357/ab4659.

P. M. W. Kalberla, W. B. Burton, D. Hartmann, E. M. Arnal, E. Bajaja, R. Morras, and W. G. L. Pöppel. The Leiden/Argentine/Bonn (LAB) Survey of Galactic HI. Final data release of the combined LDS and IAR surveys with improved stray-radiation corrections. A&A, 440(2): 775–782, Sept. 2005. doi: 10.1051/0004-6361:20041864.

KERR, F., HINDMAN, J, and CARPENTER, M. The Large-Scale Structure Of the Galaxy. *Nature*, page 3, Oct. 1957.

E. S. Levine, Leo Blitz, and Carl Heiles. THE VERTICAL STRUCTURE OF THE OUTER MILKY WAY HI DISK. AJ, page 16, Jan. 2006.

Ralph Schonrich, James Binney, and Martin Asplund. The detection and treatment of distance errors in kinematic analyses of stars. *The detection and treatment of distance errors in kinematic analyses of stars*, page 11, Aug. 2012.

Sukanya Chakrabarti and Leo Blitz. Tidal imprints of a dark subhalo on the outskirts of the Milky Way. *Monthly Notices of the Royal Astronomical Society: Letters, Volume 399, Issue 1*, page 11, Oct. 2009.

Sukanya Chakrabarti, G. Laughlin, and F. H. Shu. BRANCH, SPUR, AND FEATHER FORMATION IN SPIRAL GALAXIES. *The Astronomical Journal*, page 20, June 2003.

J. W. Wadsley, J. Stadel, and T. Quinn. Gasoline: a flexible, parallel implementation of TreeSPH. New A, 9(2):137–158, Feb. 2004. doi: 10.1016/j.newast.2003.08.004.

M. D. Weinberg and L. Blitz. A Magellanic Origin for the Warp of the Galaxy. ApJ, 641(1):L33–L36, Apr. 2006. doi: 10.1086/503607.

T. V. Wenger, D. S. Balser, L. D. Anderson, and T. M. Bania. Kinematic Distances: A Monte Carlo Method. ApJ, 856(1):52, Mar. 2018. doi: 10.3847/1538-4357/aaaec8.

Appendix

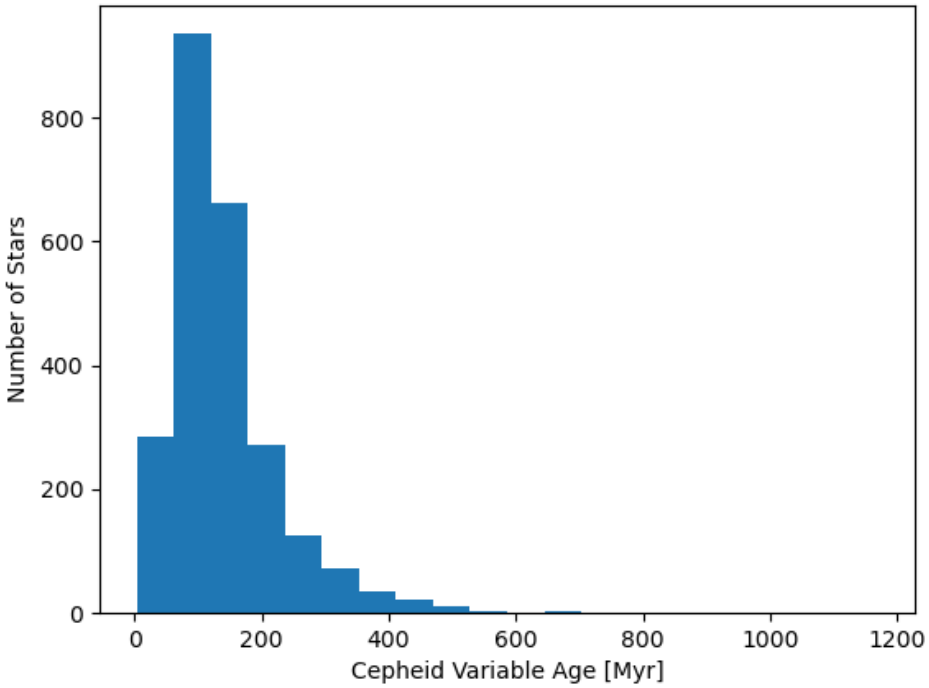

Figure 1: A histogram depicting the amount of Cepheid variables for a specific age binning. It can be seen that the majority of Cepheid variables reside between 0 and 200 Myr of age. The median of the ages was 119 with a standard deviation of 90Myr. The number of Cepheid variables falls off around 400 to 600Myr of age.

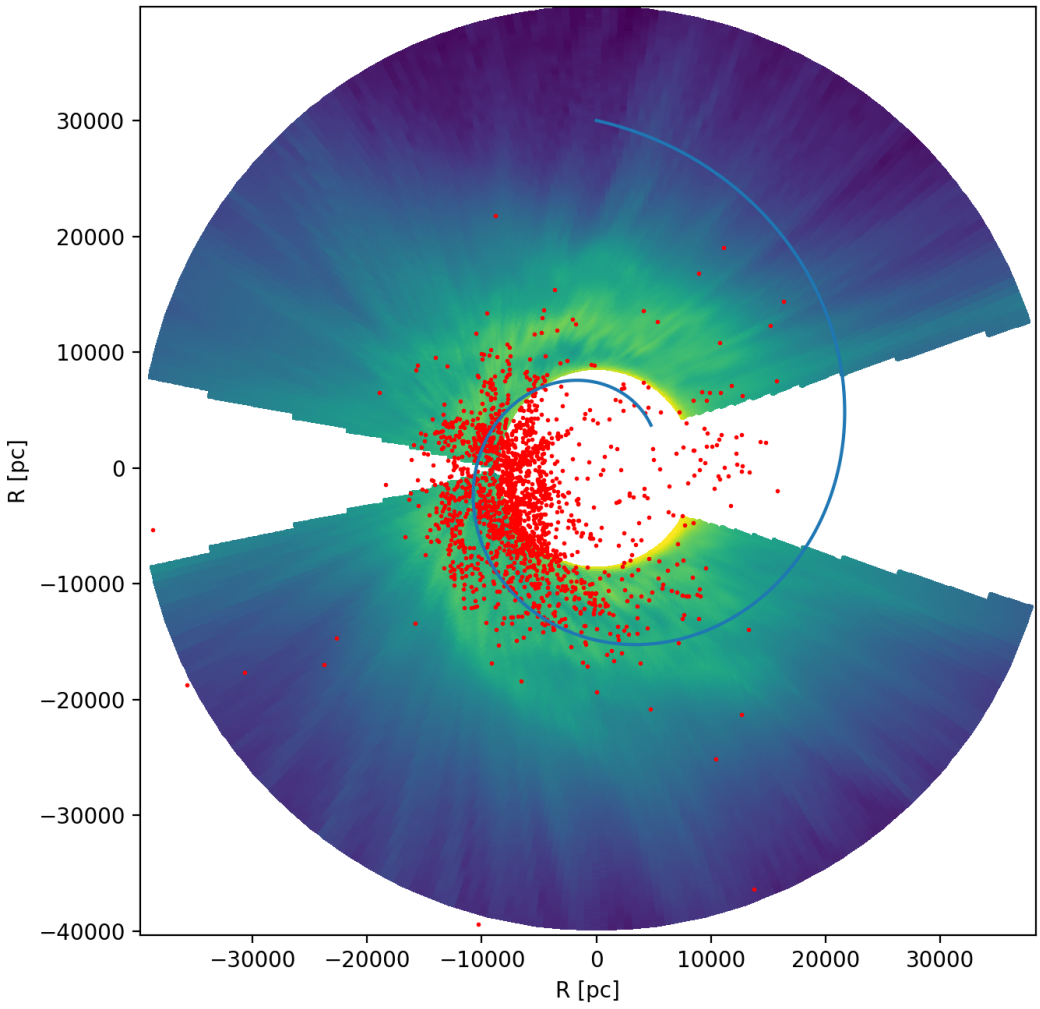

Figure 2: The topographical map of the HI in the MW with Cepheid variable stars superimposed on top. Regions in the HI map that are greener indicate a more dense region of HI. Regions in the HI map that are bluer indicate a less dense region of HI. The Cephied variable stars' positions are shown by the red points, and the spiral is shown as the blue spiral line. It is important to note that we only take the Cehpeids from 29 to 209 Gyr. This is because this range is one sigma away from the mean Cephied age value which ensures that we are able to distinguish the spiral structure these Cepheids in this age range follow.

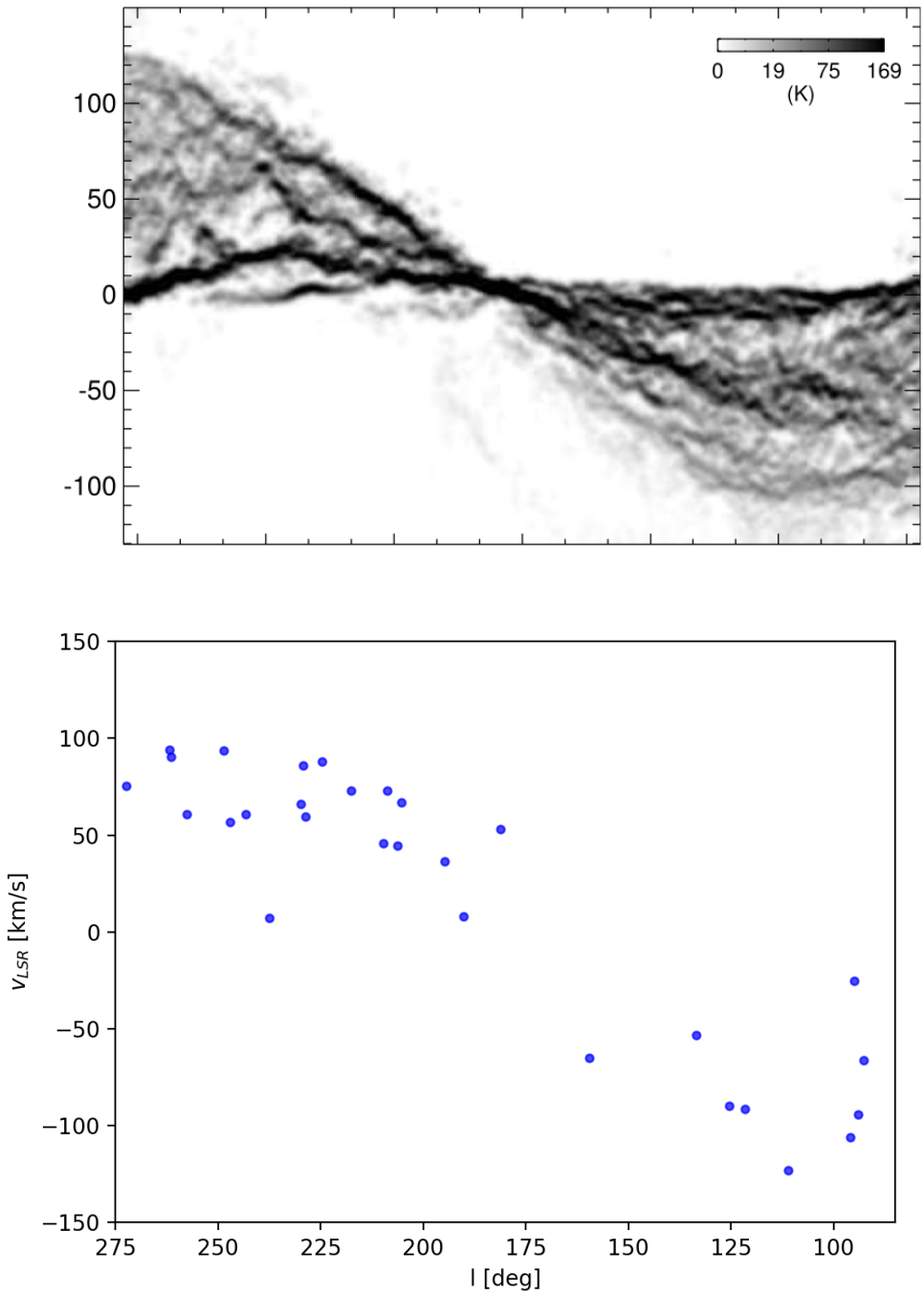

Figure 3: Top: HI (l, v_{LSR}) diagram of the Galactic plane obtained by integrating local peaks from 5^0 b to b 5^0. The gray scale represents the integrated intensity in K. This plot is from Bon-Chul Koo et al. (2017). Bottom: Each point in this plot is a star from Gaia DR3 with radial velocity information that had a listed age of less than 400Myr. This is meant to mimic the top plot.